Interferon regulatory factor-8 modulates the development of tumour-induced CD11b$^+$Gr-1$^+$ myeloid cells

Trina J. Stewart [a, #], Kristy M. Greeneltch [a, #], Julia E. Reid [a], David J. Liewehr [b], Seth M. Steinberg [b], Kebin Liu [c], Scott I. Abrams [a, d, *]

[a] *Laboratory of Tumor Immunology and Biology, National Cancer Institute, National Institutes of Health, Bethesda, MD, USA*
[b] *Biostatistics and Data Management Section, National Cancer Institute, National Institutes of Health, Bethesda, MD, USA*
[c] *Department of Biochemistry and Molecular Biology, Medical College of Georgia, Augusta, GA, USA*
[d] *Department of Immunology, Roswell Park Cancer Institute, Buffalo, NY, USA*

Received: August 18, 2008; Accepted: January 14, 2009

Abstract

Tumour-induced myeloid-derived suppressor cells (MDSC) promote immune suppression and mediate tumour progression. However, the molecular basis for the generation of MDSC, which in mice co-express the CD11b$^+$ and Gr-1$^+$ cell surface markers remains unclear. Because CD11b$^+$Gr-1$^+$ cells expand during progressive tumour growth, this suggests that tumour-induced events alter signalling pathways that affect normal myeloid cell development. Interferon regulatory factor-8 (IRF-8), a member of the IFN-γ regulatory factor family, is essential for normal myelopoiesis. We therefore examined whether IRF-8 modulated tumour-induced CD11b$^+$Gr-1$^+$ cell development or accumulation using both implantable (4T1) and transgenic (MMTV-PyMT) mouse models of mammary tumour growth. In the 4T1 model, both splenic and bone marrow-derived CD11b$^+$Gr-1$^+$ cells of tumour-bearing mice displayed a marked reduction in IRF-8 expression compared to control populations. A causal link between IRF-8 expression and the emergence of tumour-induced CD11b$^+$Gr-1$^+$ cells was explored *in vivo* using a double transgenic (dTg) mouse model designed to express transgenes for both IRF-8 and mammary carcinoma development. Despite the fact that tumour growth was unaffected, splenomegaly, as well as the frequencies and absolute numbers of CD11b$^+$Gr-1$^+$ cells were significantly lower in dTg mice when compared with single transgenic tumour-bearing mice. Overall, these data reveal that IRF-8 plays an important role in tumour-induced development and/or accumulation of CD11b$^+$Gr-1$^+$ cells, and establishes a molecular basis for the potential manipulation of these myeloid populations for cancer therapy.

Keywords: IRF-8 • myeloid-derived suppressor cells • tumour progression • haematopoiesis

Introduction

During host–tumour interactions, a variety of tumour-derived factors (TDF) serve to down-regulate T-cell responses directly or indirectly *via* recruitment of various immune suppressive cell subpopulations [1–3]. Indeed, a number of distinct immune suppressive cell subsets have been defined that inhibit adaptive T-cell-mediated immunity. For example, in mouse models, tumour growth and progression have been accompanied by the expansion and accumulation of a heterogeneous population of myeloid cells that co-express the CD11b and Gr-1 differentiation markers, and have been termed myeloid-derived suppressor cells (MDSC) [4, 5]. Although more extensively studied in animal models, the proliferation of immunosuppressive myeloid subpopulations have also been observed in human neoplasia, including carcinoma of the head and neck, non-small cell lung carcinoma, renal carcinoma, melanoma and adenocarcinomas of the colon, breast and pancreas [6–10].

In experimental animal models, tumour-induced CD11b$^+$Gr-1$^+$ cells have been implicated in the suppression of T-cell-mediated immunity through diverse pathways, including: (a) the secretion of transforming growth factor-β (TGF-β) which down-regulates CTL induction [11]; (b) the production of nitric oxide, degradation of arginine *via* arginase-1 activity or the generation of reactive oxygen species that alters signalling, activation and eventually survival of T cells [4, 5, 8, 12] and (c) the promotion of tumour angiogenesis through matrix metalloproteinase-9 (MMP-9) production [13]. Although these MDSC are readily apparent in the bone marrow

# These authors contributed equally to this study.
*Correspondence to: Scott I. ABRAMS,
Department of Immunology, Roswell Park Cancer Institute,
Elm and Carlton Streets, Buffalo, NY 14263, USA.
Tel.: (716) 845-4375
Fax: (716) 845-1322
E-mail: scott.abrams@roswellpark.org

doi: 10.1111/j.1582-4934.2009.00685.x

No claim to original US Government work
Journal compilation © 2009 Foundation for Cellular and Molecular Medicine/Blackwell Publishing Ltd

and peripheral lymphoid organs, they can also infiltrate tumour tissue and constitute approximately 5% of the total cells within the mass [13].

Multiple mechanisms have been reported to account for the immune suppressive behaviour of MDSC, including those outlined above. However, the molecular pathway(s) that underlie their development or expansion remain to be elucidated. Because $CD11b^+Gr\text{-}1^+$ MDSC aberrantly expand during the process of tumour growth, this suggests that tumour-induced events alter the signalling pathways that affect normal myeloid cell production, differentiation and/or survival. One principal gene that positively regulates normal myeloid cell development, differentiation and function in monocytes/macrophages and dendritic cells is interferon regulatory factor-8 (IRF-8). IRF-8, also known as interferon consensus sequence binding protein, is a member of the IRF family of transcription factors [14–16].

The importance of IRF-8 in regulating normal myelopoiesis has been clearly illustrated in IRF-8 null mice [17–19]. IRF-8-deficiency alters normal haematopoiesis, and leads to a marked accumulation of macrophages, neutrophils and $CD11b^+Gr\text{-}1^+$ cells in the spleen, lymph nodes, peripheral blood and bone marrow [17–19]. Additionally, IRF-8-deficient macrophages and neutrophils exhibit heightened levels of apoptotic resistance [20]. Ultimately, these mice develop a chronic myelogenous leukaemia-like syndrome [17], revealing that IRF-8 plays an integral role in the regulation of cell death and the pathogenesis of certain haematological malignancies. These observations also raise the notion that the production or accumulation of $CD11b^+Gr\text{-}1^+$ MDSC in tumour-bearing hosts arise, at least in part, as a consequence of a novel mechanism of tumour-induced IRF-8 down-regulation.

To test this hypothesis, we made use of both implantable (4T1) and transgenic (MMTV-PyMT) mouse models of mammary carcinoma. The 4T1 tumour cell line is a well characterized model, reflecting a spontaneously arising neoplasm in BALB/c mice [21–23]. When implanted orthotopically into a mammary gland of syngeneic mice, 4T1 exhibits progressive tumour growth that is accompanied by spontaneous metastasis to the lymph nodes, lung, liver, bone marrow and brain, as well as a rapid and robust accumulation of MDSC that are readily detectable in peripheral lymphoid tissues. The second model involved the use of transgenic (Tg) mice expressing the polyomavirus middle T antigen (PyMT) under the transcriptional control of the MMTV promoter [24], henceforth termed MTAG mice [25, 26]. These mice develop tissue-specific mammary gland carcinoma, which eventually metastasizes to the lungs. Tumour progression in MTAG mice has been shown to mimic human breast cancer pathology at morphological (disease stage), molecular and immunological levels [25–28]. Moreover, we recently demonstrated that autochthonous primary tumour growth in MTAG mice was accompanied by a significant accumulation of splenic $CD11b^+Gr\text{-}1^+$ cells [26]. This model has also been used to study the role of tumour-associated macrophages in tumour progression [29].

In both the 4T1 and MTAG models, we showed that tumour-induced $CD11b^+Gr\text{-}1^+$ cells displayed a marked reduction in constitutive IRF-8 expression levels compared to non-tumour-bearing control populations. Furthermore, through the use of a double Tg (dTg) mouse model, designed to harbour transgenes for both IRF-8 and mammary carcinoma development (MTAG), we observed a significant reduction in both splenomegaly and the frequencies of $CD11b^+Gr\text{-}1^+$ cells *in vivo* compared to that observed in single transgenic (sTg) tumour-bearing mice. Taken together, these data reveal an important role for IRF-8 in the development/expansion of $CD11b^+Gr\text{-}1^+$ cells during tumour progression.

Materials and methods

Mice

Female BALB/c (H-2^d) and C57BL/6 (B6; H-2^b) mice, 5–6 weeks of age, were obtained from the National Cancer Institute-Frederick Cancer Research Animal Facility (Frederick, MD, USA). Female CB6F1/J hybrid mice (BALB/cJ F $\times$ C57BL/6J M) were obtained from The Jackson Laboratory (Bar Harbor, ME, USA). The MTAG (MMTV-PyMT) transgenic mouse expresses the polyomavirus middle T antigen driven by the MMTV-LTR promoter [24]. These transgenic mice were originally derived in FVB mice [24] and were later backcrossed on a B6 background, which was kindly provided by S. Gendler (Mayo Clinic, Scottsdale, AZ, USA) [30]. Polyomavirus middle T oncogene expression results in the generation of multifocal mammary carcinomas in 100% of female mice, followed by progression to pulmonary metastases in the vast majority [24, 26]. Only female MTAG mice were used in these experiments and were obtained by breeding Tg male mice with wild-type B6 female mice. Progeny were monitored for transgene expression by PCR analysis. Non-Tg littermates were used as age- and gender-matched controls. All mice in these studies were housed in a specific pathogen-free environment, and all experiments were conducted under approved protocols in accordance with institutional guidelines for animal care and use (IACUC).

In accordance with these regulations, no single tumour mass was allowed to exceed 2 cm^3, although MTAG mice may develop up to 10 discrete tumours. MTAG mice were killed once any single tumour mass reached 2 cm^3 in size or tumours interfered with normal activity. Tumour growth was measured weekly in two dimensions, using a digital calliper, and tumour volume was calculated as previously described [26] using the formula $(w^2 \times l)/2$. In MTAG mice, total tumour volume was determined as the sum of each distinct tumour volume within an individual mouse.

Production of IRF-8 Tg mice

Complementary DNA (cDNA) encoding the mouse IRF-8 coding sequence was cloned into the pcDNA3.1(+) plasmid (Invitrogen, Carlsbad, CA, USA) under the control of the cytomegalovirus (CMV) promoter (plasmid kindly provided by K. Ozato, National Institutes of Health [NIH], Bethesda, MD, USA). A 4.3-kb fragment was then generated from the construct by cleavage at an FspI restriction site, and isolation by sucrose gradient purification. This purified material was then microinjected into the pronuclei of one cell embryos of fertilized eggs from B6 mice to obtain several founder mice (Laboratory Animal Sciences Program, SAIC, Frederick, MD, USA). Transgene integration in progeny was verified by Southern blot analysis using the 4.3-kb fragment as the probe and PCR genotyping of tail snips. The founder line, E5, was selected for this study based on the highest IRF-8

No claim to original US Government work
Journal compilation © 2009 Foundation for Cellular and Molecular Medicine/Blackwell Publishing Ltd

copy number and mRNA levels. Furthermore, no atypical effects of IRF-8 transgene expression were observed on various haematological parameters, as determined by phenotypic analysis of the spleen and complete blood count (CBC) on peripheral whole blood. F1 progeny were produced by mating sTg male mice with either wild-type female B6 or BALB/c mice. Moreover, male MTAG mice were bred with female IRF-8 Tg mice to produce dTg mice (in a B6 background) that possessed the transgenes for both IRF-8 and spontaneous mammary carcinoma development (*i.e.* MMTV-PyMT). Transgene expression was verified by PCR analysis of tail snip DNA using the conditions mentioned in the PCR/RT-PCR section below.

Tumour cells and inoculations

The 4T1 mammary carcinoma cell line was obtained from the American Type Culture Collection (CRL-2539; ATCC, Manassas, VA, USA). 4T1 cells were maintained in RPMI supplemented with 0.1 mM non-essential amino acids, 1mM sodium pyruvate, 2 mM L-glutamine, 15 mM HEPES, 100 U/ml penicillin-100 μg/ml streptomycin solution, 50 μM 2-mercaptoethanol and 10% heat inactivated foetal bovine serum (Gemini, Woodland, CA, USA). 4T1 tumour growth was achieved *in vivo* by orthotopic implantation of 4T1 cells (5×10^4 cells) into mammary gland #2. Tumour growth was measured thrice weekly in two dimensions, using a digital calliper, and tumour volume calculated as noted earlier. Mice were euthanized 20–27 days after injection, and spleens and/or bone marrow cells were collected by flushing the femurs and tibias with culture medium, as previously described [31].

Flow cytometric studies

All antibodies (Ab) utilized in these experiments were purchased from BD Biosciences (San Diego, CA, USA). Unfractionated splenocytes or bone marrow cells were stained by direct immunofluorescence with anti-CD11b-PE, anti-Gr-1-FITC, anti-B220-FITC, anti-CD4-PE, anti-CD8-FITC mAb or the appropriate isotype-matched Ab controls, as described [26] and analysed by flow cytometry using a FACSCalibur flow cytometer (Becton Dickinson, San Jose, CA, USA). Data were analysed by CellQuest software (Becton Dickinson).

Purification and culture of $CD11b^+Gr\text{-}1^+$ cells

$CD11b^+Gr\text{-}1^+$ cells were purified from the spleens or bone marrow of control or tumour-bearing mice using similarly established protocols [32]. Briefly, single cell suspensions were suspended in 'depletion buffer' (PBS, pH 7.2, containing 2 mM ethylenediaminetetraacetic acid and 0.5% bovine serum albumin) before the addition of anti-CD11b MicroBeads (Miltenyi Biotec, Auburn, CA, USA), as per manufacturer's instructions. Cells were maintained on ice for 30 min., followed by washing with a 15–20 fold (v/v) excess of the same buffer. Cells were then resuspended to an appropriate volume and passed through a MACS pre-separation filter prior to separation on the AutoMACS separator system (Miltenyi Biotec) using a double column depletion protocol. Purity of the positively selected myeloid population was ascertained using anti-CD11b-PE and anti-Gr-1-FITC mAb, as previously outlined. This technique was very effective for the isolation of $CD11b^+$ cells that also co-expressed Gr-1, resulting in populations of double-positive cells that were routinely >90% from both control and tumour-bearing (4T1, MTAG) mice. (In many cases, the purity was even greater.) $CD11b^+Gr\text{-}1^+$ cells were stimulated by culturing for 24 hrs in the absence or presence of lipopolysaccharide (LPS/L-6143; Sigma-Aldrich, St. Louis, MO, USA) and recombinant mouse IFN-γ (100 U/ml; R&D Systems, Minneapolis, MN, USA). Cell-free supernatants were then collected for cytokine analysis, and the cells retrieved for RNA isolation.

Proliferation assay

Ninety-six-well flat-bottomed plates were pre-coated with anti-CD3 mAb (1 μg/well) by incubation at 4°C overnight; plates were then washed prior to the addition of the various cell combinations. Splenic $CD4^+$ or $CD8^+$ T cells were purified from CB6F1/J hybrid mice (using T cell subset-specific MicroBeads and the AutoMACS separator, and plated (5×10^4 cells/well). Splenic $CD11b^+Gr\text{-}1^+$ cells were purified, as described above, from the non-tumour-bearing control or 4T1 tumour-bearing hybrid mice and added to the plate at a $CD11b^+Gr\text{-}1^+$ cell : T-cell ratio of 1:1. Plates were incubated for 48 hrs at 37°C, after which ^{3}H-thymidine (1 μCi/ well) was added for an additional 24 hrs of culture. The extent of proliferation was determined by measuring ^{3}H-thymidine incorporation by liquid scintillation spectroscopy.

RT-PCR and PCR analyses

For RT-PCR, total RNA was isolated from $CD11b^+Gr\text{-}1^+$ cells using RNeasy Mini kits from Qiagen (Valencia, CA, USA) according to manufacturer's instructions. The RNeasy kit includes a silica-membrane technology that efficiently removes genomic DNA without DNase treatment. Total RNA was used for first strand cDNA synthesis using the ThermoScript RT-PCR system (Invitrogen). The cDNA was then used as the template for PCR amplification of the following mouse genes: GAPDH, IRF-8, IL-12p40 and inducible nitric oxide synthase (iNOS). PCR reactions were carried out in a PTC-200 thermal cycler (MJ Research, Waltham, MA, USA) under the following conditions: 94°C for 2 min., 30 cycles (94°C for 30 sec., 60°C for 30 sec. and 72°C for 1 min.) and 72°C for 10 min. The PCR primers for GAPDH were as follows: forward primer: 5′-CATCACCATCTTCCAGGAGCG-3′; reverse primer: 5′-ACGGACACATTGGGGGTAGG-3′. The PCR primers for IRF-8 were as follows: forward primer: 5′-CGTGGAAGACGAGGTTACGCTG-3′; reverse primer: 5′- GCTGAATGGTGTGTGTCATAGGC-3′. The PCR primers for IL-12p40 were as follows: 5′-TCACCTGCCCAACTGCCGAG-3′; reverse primer: 5′-GGAACGCACCTTTCTGGTTACAC-3′. The PCR primers for iNOS were as follows: forward primer: 5′-CCAGAGGACCCAGAGACAAGC-3′; reverse primer: 5′-GGCAGCACATCAAAGCGGC-3′. For PCR analysis, various cycle numbers were previously tested, and 30 cycles was found to be optimal for effectively distinguishing differences in IRF-8 levels between control and tumour-induced $CD11b^+Gr\text{-}1^+$ cells. For genotyping transgenic offspring, PCR analysis was performed with the same IRF-8 primers (30 cycles), which effectively distinguished transgenic IRF-8 levels from endogenous genomic IRF-8 levels (the latter of which were undetectable under these conditions), while the PCR primers (40 cycles) for PyMT were as follows: forward primer: 5′-AGTCACTGCTACTGCACCCAG-3′; reverse primer: 5′-CTCTCCTCAGTTCCTCGCTCC-3′. PCR products were separated on a 1% or 2% agarose gel, and images captured with the BioDocIt imaging system (UVP, Upland, CA, USA).

To quantify PCR band intensities, gel images were first captured as noted above. The PCR band intensity was then quantified using the NIH Image J program (NIH). The IRF-8 band intensity of each sample was

No claim to original US Government work
Journal compilation © 2009 Foundation for Cellular and Molecular Medicine/Blackwell Publishing Ltd

normalized over the band intensity of GAPDH corresponding to that same sample. The relative IRF-8 level was expressed as the IRF-8 band intensity/GAPDH band intensity.

Statistical analysis

Two pairwise comparisons were performed to compare distributions of the wild-type (double-negative) *versus* IRF-8 Tg genotypes, or the sTg (MTAG) *versus* dTg genotypes for each parameter. For comparisons of the wild-type *versus* IRF-8 Tg genotypes, or tumour volumes between the sTg (MTAG) and dTg genotypes, ANOVA was used to perform the analysis, with the litter specified as the experimental unit. For other comparisons of sTg (MTAG) *versus* dTg genotypic parameters, an analysis of covariance was performed, with the litter specified as the experimental unit and tumour volume as the covariate, since the association varied with volume. Specifically, comparisons between genotypes were made at the quartiles of tumour volume if the volume was related to the given parameter. This covariate was dropped from the model only if both slope estimates were equal to zero, in which case the model was reduced to an ANOVA analysis such as for the comparison of the wild-type *versus* IRF-8 Tg genotypes. Tumour-induced $CD11b^+Gr\text{-}1^+$ data were analysed with a mixed model ANOVA; treatment (control *versus* 4T1-bearing mice) was the fixed effect and mouse and sample ('triplicate') were the random effects. Two-sample comparisons were performed with a t-test (after verifying normality of distributions). Given the number of analyses performed and the likely relatedness of parameters, only a P-value < 0.01 was considered statistically significant, while P-values between 0.01 and 0.05 would be associated with strong trends.

Results

Accumulation of $CD11b^+Gr\text{-}1^+$ cells in the spleen and bone marrow of tumour-bearing mice

$CD11b^+Gr\text{-}1^+$ cells are found at low frequencies in the spleens of wild-type mice. However, these cells have been shown to expand extensively with progressive tumour growth [4, 5, 8, 12, 22]. To understand the relationship between IRF-8 expression and the expansion of $CD11b^+Gr\text{-}1^+$ cells in tumour-bearing hosts, we examined two models, reflecting implantable (4T1 mammary carcinoma) or autochthonous (MTAG) tumour growth. In the implantable tumour setting, 4T1 cells were injected orthotopically into the mammary gland of female BALB/c or CB6F1/J ($H\text{-}2^{b/d}$) hybrid mice, and tumour measurements recorded. Age-matched control mice did not receive a tumour injection. In the MTAG model, female sTg mice with varying tumour loads (from approximately 1.3–2.5 cm^3 total tumour volume) were compared with age-matched, littermate wild-type mice (*e.g.* see Fig. 6A).

A robust accumulation of $CD11b^+Gr\text{-}1^+$ cells was observed in the spleens of 4T1 tumour-bearing mice (Fig. 1A). The results from the five mice illustrated are representative of several independent experiments in two different strains of $H\text{-}2^d$-expressing mice. Based on analysis of the five separate mice represented, the percentages of $CD11b^+Gr\text{-}1^+$ cells in the spleen ranged from 29–44% (Fig. 1A, left panel), which translated to approximately $150–300 \times 10^6$ total $CD11b^+Gr\text{-}1^+$ cells/spleen (Fig. 1B, right panel). Values for splenic $CD11b^+Gr\text{-}1^+$ cells in non-tumour-bearing mice ranged from 1% to 4%. Moreover, analysis of bone marrow cells in a separate group of 4T1 tumour-bearing mice revealed increases in both the percentages ($P = 0.011$) and absolute numbers ($P = 0.037$) of $CD11b^+Gr\text{-}1^+$ cells as compared to non-tumour-bearing control preparations (Fig. 1B). Representative dot plot analyses of $CD11b^+Gr\text{-}1^+$ cells from unfractionated spleen and bone marrow compartments of both control and 4T1 tumour-bearing mice are also illustrated (Fig. 2). Functional studies revealed that tumour-derived $CD11b^+Gr\text{-}1^+$ cells inhibited TCR-induced proliferation of $CD4^+$ or $CD8^+$ T cells compared to $CD11b^+Gr\text{-}1^+$ cells of non-tumour-bearing control mice (Fig. 1C), an important characteristic of MDSC. These data also support our previous findings in the MTAG model [26], where we observed analogous results in terms of splenomegaly and alterations in the frequencies and numbers of $CD11b^+Gr\text{-}1^+$ cells as a consequence of autochthonous tumour growth (see also Figs. 5 and 6). In addition, despite the considerable expansion of splenic $CD11b^+Gr\text{-}1^+$ cell populations, no significant changes were observed in the absolute numbers of various other lymphocyte subsets between MTAG mice with extensive tumour burdens *versus* non-tumour-bearing littermate control mice [26].

IRF-8 is down-regulated in tumour-induced $CD11b^+Gr\text{-}1^+$ cells

One possibility for the robust expansion or accumulation of tumour-induced $CD11b^+Gr\text{-}1^+$ cells is altered myelopoiesis. Because IRF-8 is crucial for maintaining normal myelopoiesis [14–19], we examined whether IRF-8 expression was altered in 4T1 tumour-induced $CD11b^+Gr\text{-}1^+$ cells. $CD11b^+$ cells were purified from the spleens or bone marrow of control and 4T1 tumour-bearing mice. We developed a highly effective technique for the isolation of $CD11b^+$ cells that co-expressed Gr-1 from both control and tumour-bearing (4T1, MTAG) mice. These purified $CD11b^+Gr\text{-}1^+$ cells were then evaluated for IRF-8 expression levels after treatment with or without IFN-γ/LPS (Fig. 3A and B). IFN-γ/LPS were used to optimally up-regulate IRF-8 expression, as previously described [18, 33]. In some experiments, cell-free supernatants were recovered for cytokine analysis (Fig. 3C and D).

In the five separate tumour-derived $CD11b^+Gr\text{-}1^+$ preparations analysed in Fig. 1, we observed a reproducible reduction of both basal and inducible IRF-8 expression levels as compared to the control preparation (Fig. 3A, upper left and right panels). Due to the low frequencies of $CD11b^+Gr\text{-}1^+$ cells in non-tumour bearing control mice, RNA was extracted from $CD11b^+Gr\text{-}1^+$ cells that were isolated from a pool of five control spleens, and was representative of several independent experiments (*e.g.* see Fig. 3A, lower panel as another independent experiment). The expression of iNOS was measured as a positive control for cellular activation.

No claim to original US Government work
Journal compilation © 2009 Foundation for Cellular and Molecular Medicine/Blackwell Publishing Ltd

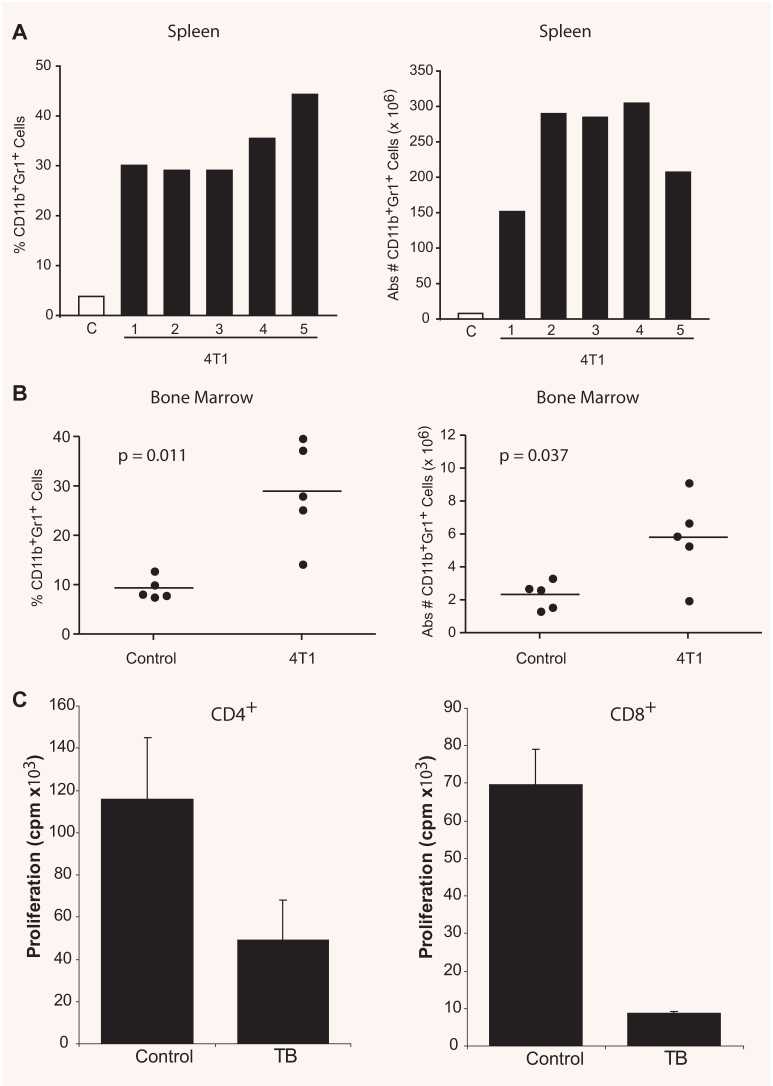

Fig. 1 Accumulation of $CD11b^+Gr\text{-}1^+$ cells in 4T1 tumour-bearing mice. 4T1 mammary tumour cells (5×10^4/mouse) were injected orthotopically in five individual female CB6F1/J ($H\text{-}2^{b/d}$) mice. Control (denoted as 'C') mice did not receive a tumour injection. Upon reaching the ethical limit of 2 cm^3 tumour volume (at day 26), all mice were euthanized, and splenocytes recovered for enumeration. (**A**, left panel) Unfractionated splenocytes were evaluated for the percentage of $CD11b^+Gr\text{-}1^+$ cells using two-colour flow cytometry. (**A**, right panel) Absolute numbers of $CD11b^+Gr\text{-}1^+$ cells were calculated by multiplying the percentages determined in (**A**) by total splenocyte counts. For both panels, splenocytes from the control group were pooled and an average result determined, whereas splenocytes from the 4T1 tumour-bearing mice were analysed separately. Comparable results were observed when BALB/c mice were similarly challenged with 4T1 cells. In a separate experiment, the percentages (**B**, left panel) and absolute numbers (**B**, right panel) of $CD11b^+Gr\text{-}1^+$ cells were determined, as described above from unfractionated bone marrow cells of control and 4T1 tumour-bearing mice. Each data point represents the results of an individual mouse. (**C**) Splenic $CD4^+$ or $CD8^+$ T cells were purified from non-tumour-bearing wild-type (WT) CB6F1/J mice. T cells were mixed with $CD11b^+Gr\text{-}1^+$ cells purified from the spleens of either WT or 4T1 tumour-bearing (TB) CB6F1/J mice (1:1 ratio). In the case of the control group, both T cells and $CD11b^+Gr\text{-}1^+$ cells were obtained from the same mouse. In the case of tumour-induced $CD11b^+Gr\text{-}1^+$ cells, T cells from a wild-type mouse were used to avoid any *in vivo* tumour-induced effect on T-cell function. Cultures were then incubated in the absence or presence of immobilized anti-CD3 mAb for 48 hrs. Proliferation was measured by ^{3}H-thymidine uptake after an additional 24 hrs of incubation. Results represent the mean ± S.E.M. of triplicate wells.

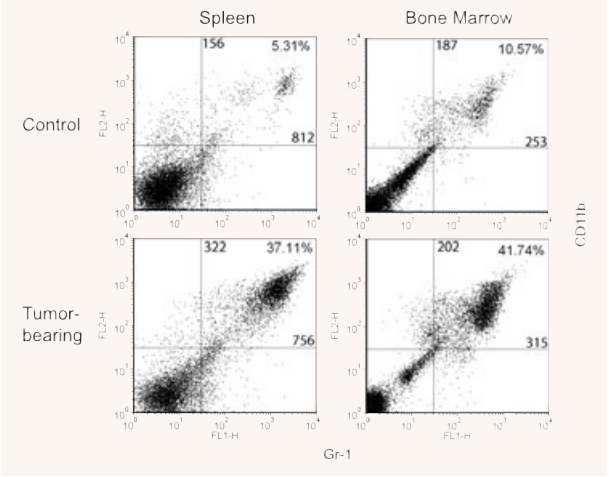

Fig. 2 Flow cytometric analysis of $CD11b^+Gr\text{-}1^+$ cells from both spleen and bone marrow of control and 4T1 tumour-bearing mice. Representative two-colour dot plots for the percentages and MFI values of $CD11b^+Gr\text{-}1^+$ cells derived from Fig. 1. The percentages and MFI values for two-colour staining are shown in the upper right quadrant. The MFI values for CD11b and Gr-1 staining are shown along the vertical and horizontal lines within the upper right quadrant, respectively. Data are representative of at least five separate mice per group.

No claim to original US Government work
Journal compilation © 2009 Foundation for Cellular and Molecular Medicine/Blackwell Publishing Ltd

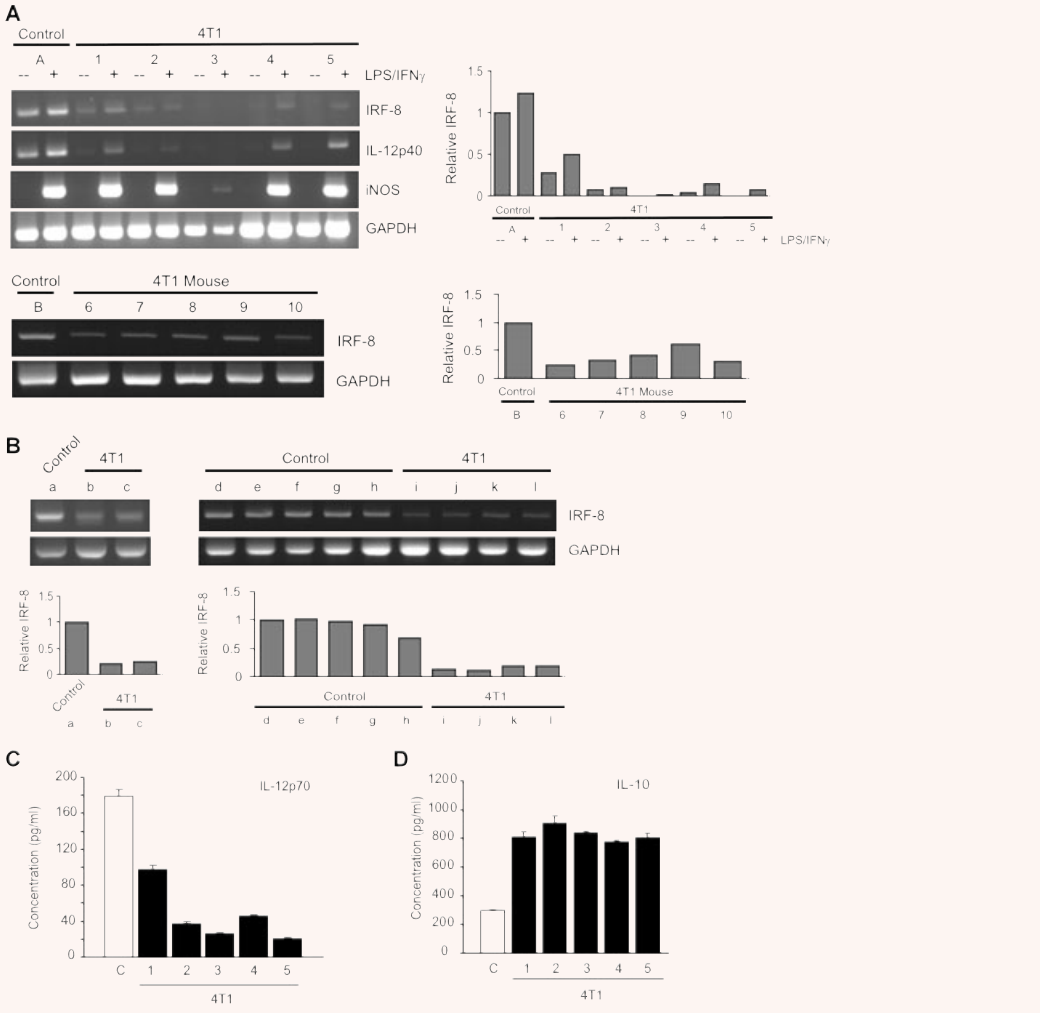

Fig. 3 IRF-8 expression is down-regulated in 4T1 tumour-induced CD11b$^+$Gr-1$^+$ cells. CD11b$^+$Gr-1$^+$ cells from the control and 4T1 tumour-bearing groups of mice shown in Fig. 1 were analysed for the expression of the indicated genes by RT-PCR (upper set of genes corresponds to **A**). CD11b$^+$Gr-1$^+$ cells were first purified by CD11b-magnetic bead cell separation, and incubated overnight in the absence (−) or presence (+) of IFN-γ (100 U/ml) plus LPS (1 μg/ml). (Mouse #3 showed a weak response to iNOS induction, but responded as well as the other 4T1-tumour-bearing mice in terms of IL-10 production; see **D**). (Lower gel of **A**) In a separate experiment, IRF-8 expression levels were determined, as described above, from a control group ('B') and five individual tumour-bearing mice ('6–10'). Control CD11b$^+$Gr-1$^+$ cells were first collected from a pool of splenocytes, whereas CD11b$^+$Gr-1$^+$ cells from 4T1 tumour-bearing mice were isolated from individual mice. Experiments were repeated in BALB/c mice with similar results. (**B**) IRF-8 expression levels of CD11b$^+$Gr-1$^+$ cells purified from bone marrow of control (a; d–h) and 4T1 tumour-bearing CB6F1/J mice (b, c; i–l), as in (**A**). The results are summarized from two independent experiments shown as, 'a–c' and 'd–l'. Samples shown as 'd–l' represent data from individual mice, whereas samples shown as 'a, b and c' represent data from pools of five, two and two mice, respectively. The relative levels of IRF-8 shown in (**A**) and (**B**) were quantified by analysis of the PCR band intensities, as described in the 'Materials and methods'. The first lane of each of the four gels was arbitrarily set at a relative intensity of 1. (**C** and **D**) Tumour-induced CD11b$^+$Gr-1$^+$ cells also displayed an altered IL-12/IL-10 profile. CD11b$^+$Gr-1$^+$ cells of the same control ('C') and 4T1 tumour-bearing groups shown in (**A**) were also analysed for production of IL-12 (IL-12p70) and IL-10 following stimulation with IFN-γ and LPS overnight. Cytokines were undetectable in the absence of stimulation (not shown). Data represent the mean ± S.E.M. of triplicate determinations for cytokine concentration from each preparation. Experiments were repeated in BALB/c mice with similar results.

In addition, because IL-12p40 subunit expression is IRF-8 dependent [18, 33], we examined control and tumour-induced CD11b$^+$Gr-1$^+$ cells for alterations in IL-12p40 expression levels. As with IRF-8, we observed a reduction in IL-12p40 expression levels in CD11b$^+$Gr-1$^+$ cells from tumour-bearing mice compared with control cells. These latter findings also validated that the reduction in IRF-8 expression levels were significant enough to have downstream functional significance. A reduction

No claim to original US Government work
Journal compilation © 2009 Foundation for Cellular and Molecular Medicine/Blackwell Publishing Ltd

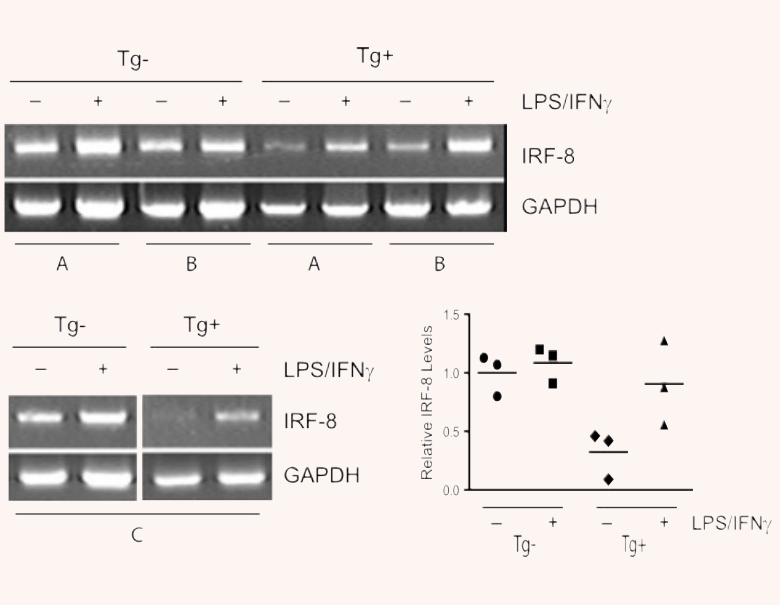

Fig. 4 IRF-8 expression is reduced in CD11b$^+$Gr-1$^+$ cells derived from tumour-bearing MTAG mice. CD11b$^+$Gr-1$^+$ cells from control and tumour-bearing MTAG mice were analysed for basal and inducible IRF-8 expression levels, as in Fig. 2. CD11b$^+$Gr-1$^+$ cells were purified and then incubated overnight in the absence (−) or presence (+) of IFN-γ plus LPS. Here, three separate pairs of age-matched control ('Tg$^-$') and tumour-bearing MTAG mice ('Tg$^+$') (total tumour volume of each mouse, ≥2 cm^3), was assessed, indicated as pairs (**A**), (**B**) (upper gel) or (**C**) (lower gel). (Lower right panel) The relative levels of IRF-8 shown for mouse pairs (**A**)–(**C**) were then quantified by analysis of the PCR band intensities, as in Fig. 2. We divided (or standardized) each individual ratio (IRF-8/β-actin) by the mean ratio of the Tg- group (without *in vitro* treatment) to yield a relative ratio. The graph depicts the relative ratio for each of the twelve observations ($n = 3$ corresponding to groups **A**, **B** and **C**/*in vitro* treatment). The horizontal lines indicate the means of the standardized values.

in constitutive IRF-8 expression levels in tumour-induced CD11b$^+$Gr-1$^+$ cells, compared to the control cells, was verified in a second independent experiment (Fig. 3A, lower left and right panels). We also observed that CD11b$^+$Gr-1$^+$ cells of tumour-bearing MTAG mice displayed lower IRF-8 levels, particularly basal expression ($P = 0.011$), with respect to age-matched controls (Fig. 4).

The analysis of IRF-8 expression was extended to CD11b$^+$Gr-1$^+$ cells isolated from the bone marrow of individual 4T1 tumour-bearing or control mice. Basal IRF-8 levels of CD11b$^+$Gr-1$^+$ cells purified from the bone marrow of tumour-bearing mice (Fig. 3B, mice b and c; i–l) were found to be greatly reduced compared to controls (Fig. 3B, mice a; d–h). In all cases, IRF-8 expression levels of the controls were similar to each other (Fig. 3B, mice a, d–h) and consistently higher than those observed in samples from tumour-bearing mice (Fig. 3B upper and lower panels, a *versus* b or c; d–h *versus* i–l). Therefore, in this 4T1 model, the data indicated that IRF-8 expression within tumour-induced CD11b$^+$Gr-1$^+$ cells were demonstrably lower when compared with control preparations from both the splenic and bone marrow compartments.

After observing that IL-12p40 expression levels were reduced (Fig. 3A, top panel), we examined whether IRF-8 down-regulation correlated with a decrease in the production of IL-12 protein levels. The cell-free supernatants from the same untreated and IFN-γ/LPS-treated cell preparations were analysed, which revealed that tumour-induced CD11b$^+$Gr-1$^+$ cells produced lower amounts of IL-12 when compared with cells from control mice ($P = 0.015$; Fig. 3C). Conversely, these tumour-induced CD11b$^+$Gr-1$^+$ cells (including mouse 3) secreted significantly higher levels of IL-10, a MDSC-associated cytokine [34, 35], compared with control cells ($P = 0.009$; Fig. 2D), which verified that these preparations were functionally intact, but biologically altered.

Transgenic expression of IRF-8 reduces the accumulation of tumour-induced CD11b$^+$Gr-1$^+$ cells

Thus far, these data indicate an inverse correlation between IRF-8 levels and the emergence of tumour-induced CD11b$^+$Gr-1$^+$ cells. To establish a causal link between IRF-8 expression levels, tumour growth and the accumulation of CD11b$^+$Gr-1$^+$ cells, we developed and utilized an IRF-8 Tg mouse. Because of the role that IRF-8 plays in myelopoiesis, we postulated that transgene expression of IRF-8 in the CD11b$^+$Gr-1$^+$ cellular compartment would render these cells more refractory or resistant to tumour-induced alterations. Control experiments verified that IRF-8 expression levels were at least two-fold higher in CD11b$^+$Gr-1$^+$ cells of IRF-8 transgenic mice compared with age- and gender-matched wild-type mice (data not shown). Furthermore, a CBC with differential was performed on peripheral blood from both IRF-8 transgenic and age/gender-matched wild-type mice as readouts for potential haematopoietic changes caused by IRF-8 transgene expression (Table 1). Overall, we found that all haematological parameters measured within the leucocyte compartment of both groups of mice were within normal range. Although some fluctuations were noted in red blood cell numbers, this occurred in both groups of mice. Furthermore, no red blood cell (*e.g.* red cell mass) or platelet abnormalities were observed in both groups of mice by blood smear analysis. These data support earlier phenotypic

No claim to original US Government work
Journal compilation © 2009 Foundation for Cellular and Molecular Medicine/Blackwell Publishing Ltd

Table 1 Haematological parameters in peripheral blood of wild-type versus IRF-8 transgenic mice[a]

Cell type	Wild-type mouse #			IRF-8 transgenic mouse #			Normal range
	1	2	3	1	2	3	
Absolute numbers[b]							
Total leucocytes	4.86	6.10	3.74	5.96	6.60	6.04	1.8–10.7
Neutrophils	0.80	1.29	0.77	1.23	1.65	1.09	0.1–2.4
Lymphocytes	3.80	4.46	2.82	4.59	4.74	4.70	0.9–9.3
Monocytes	0.26	0.34	0.15	0.13	0.20	0.24	0.0–0.4
Eosinophils	0.00	0.00	0.00	0.00	0.01	0.00	0.0–0.2
Basophils	0.00	0.00	0.00	0.00	0.00	0.00	0.0–0.2
Erythrocytes	9.58 [c]	9.30	6.32	8.15	9.45	9.69	6.36–9.42
Platelets	2036.00	1049.00	1087.00	989.00	1250.00	1076.00	592–2972
Percentages							
Neutrophils	16.38	21.13	20.66	20.68	24.98	18.08	6.6–38.9
Lymphocytes	78.20	73.16	75.30	77.02	71.88	77.86	55.8–91.6
Monocytes	5.32	5.63	3.92	2.22	3.04	3.96	0.0–7.5
Eosinophils	0.06	0.00	0.08	0.07	0.10	0.08	0.0–3.9
Basophils	0.03	0.08	0.04	0.00	0.00	0.02	0.0–2.0

[a] CBC was performed on both wild-type and IRF-8 transgenic mice, which were gender- (male), age- (16–20 weeks) and littermate matched. Three mice per group were analysed.
[b] All values are enumerated as ($\times 10^{-3}/\mu l$) except for erythrocytes, which are quantified as ($\times 10^{-6}/\mu l$).
[c] Underlined values are mildly out of normal range, although no abnormalities were observed in red cells by blood smear analysis.

studies, which revealed no overt differences in the frequencies and absolute numbers of major splenic leucocyte subsets (*e.g.* T-cell subsets, B cells and myeloid populations) from IRF-8 transgenic *versus* wild-type mice (data not shown).

To evaluate the *in vivo* effects of IRF-8 transgene expression on tumour growth and $CD11b^+Gr\text{-}1^+$ development/accumulation, dTg mice were produced that expressed the transgenes for both IRF-8 and mammary carcinoma development (MTAG). To do so, we mated sTg IRF-8 and MTAG mice, which shared the same genetic background. Since sTg IRF-8 and MTAG mice are maintained as heterozygous colonies, this also allowed us to examine the resultant progeny from four possible genotypes in an age-, gender-, and in most instances, a littermate-matched manner, including those that were: dTg (*i.e.* double-positive), wild-type (double-negative) or sTg for either IRF-8 or MTAG (*i.e.* single-positive). Within these various genotypes, we focused on potential differences in the myeloid compartment, including total splenocyte counts and the percentages and absolute numbers of splenic $CD11b^+Gr\text{-}1^+$ cells.

Transgenic expression of IRF-8 was found to have a significant impact on constraining splenomegaly and $CD11b^+Gr\text{-}1^+$ myelopoiesis (Figs. 5 and 6) during autochthonous tumour growth in the dTg mice. It was observed that spleen size and total splenocyte numbers ($P = 0.007$) were significantly lower in dTg mice, compared to sTg MTAG mice (Fig. 5). The number of splenocytes in dTg mice was also not significantly different from that of wild-type ($P = 0.076$) or IRF-8 Tg ($P = 0.10$) mice (Fig. 5). This contrasts sharply with the highly significant differences noted in spleen size and splenocyte number ($P < 0.0001$) of sTg MTAG mice compared with the wild-type controls. Also, compared to the wild-type controls, IRF-8 expression alone did not significantly affect spleen size, spleen number ($P = 0.70$; Fig. 5) or the composition of various leucocyte subsets (data not shown). However, no significant ($P = 0.37$) alteration in the growth of primary mammary gland carcinoma was observed between dTg mice (2240 ± 268 mm^3) and sTg MTAG mice (1950 ± 179 mm^3), based on the tumour size data illustrated in Fig. 6A. Collectively, these observations suggested that transgenic expression of IRF-8 in dTg tumour-bearing mice resulted in a splenic phenotype similar to that of the non-tumour-bearing control mice. Furthermore, the finding that tumour size was not different between these two genotypes indicated that IRF-8 in dTg mice played an important role in

No claim to original US Government work
Journal compilation © 2009 Foundation for Cellular and Molecular Medicine/Blackwell Publishing Ltd

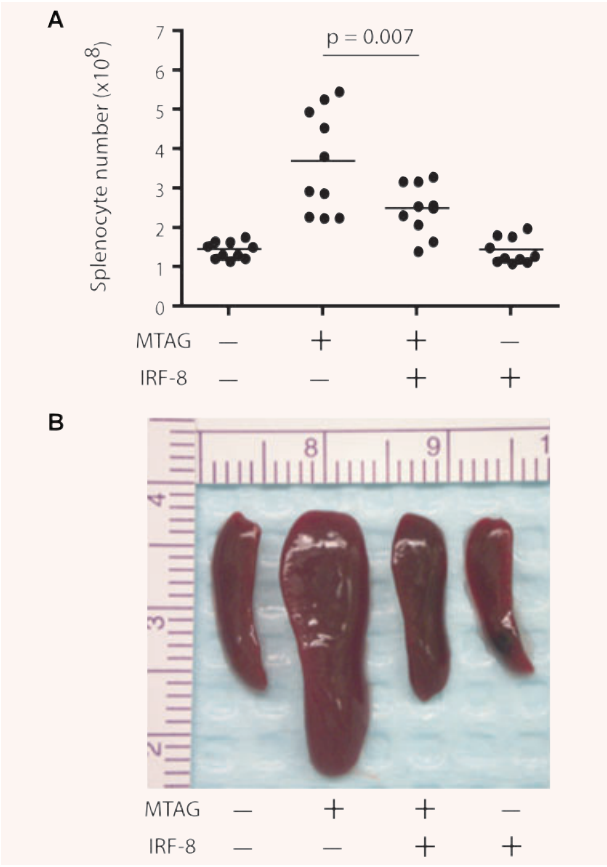

Fig. 5 Transgenic expression of IRF-8 reduces splenomegaly in a spontaneous tumour model of mammary carcinoma. (**A**): The role of IRF-8 on tumour-induced splenomegaly was analysed in a dTg mouse model designed to express the transgenes for both IRF-8 and MMTV-PyMT (denoted as MTAG). Four possible genotypes were produced as a result of mating the two heterozygous sTg mouse colonies. Transgenic expression of IRF-8 did not significantly affect primary tumour growth in dTg mice (2240 ± 268 mm^3; mean ± S.E.M. of 10 separate mice), compared with sTg MTAG mice (1950 ± 179 mm^3; $n = 10$). Mice were then killed and splenocyte counts determined alongside age- and (in most cases) littermate-matched double-negative (wild-type) or sTg IRF-8 cohorts. Each data point represents total splenocyte counts from an individual mouse. (**B**) Photographic illustration of a representative spleen of 10 mice, reflecting the four different genotypes.

providing resistance to tumour-induced splenomegaly and increased splenic cell number.

Lastly, we evaluated changes in splenocyte number in further detail, as well as the frequencies and absolute numbers of splenic $CD11b^+Gr\text{-}1^+$ cells as a function of tumour load in sTg MTAG *versus* dTg mice (Fig. 6). As demonstrated by the slope of the lines, increasing tumour volume was accompanied by a significant increase in the overall number of splenocytes ($P = 0.0007$), as well as in the number ($P = 0.013$) and percentage ($P = 0.002$) of $CD11b^+Gr\text{-}1^+$ cells in sTg MTAG mice. In contrast, increasing tumour volume had no significant effect on the total number of splenocytes ($P = 0.18$) or the number ($P = 0.62$) and percentage ($P = 0.75$) of splenic $CD11b^+Gr\text{-}1^+$ in dTg mice (Fig. 6). Thus, in dTg mice, the slope of the line remained essentially unchanged despite increases in overall tumour burden. Therefore, using these particular parameters, as tumour volume increased, so did the differences between the two tumour-bearing genotypes (Fig. 6B). For instance, when tumour volume remained low, no significant differences were observed between these two genotypes in terms of the number of splenocytes or the percentages and numbers of splenic $CD11b^+Gr\text{-}1^+$ cells (Fig. 6B). However, as tumour volume increased to intermediate and high levels, so did the significance of the differences between these two genotypes in those same haematopoietic parameters (Fig. 6B). Therefore, splenomegaly in sTg MTAG mice was the result of $CD11b^+Gr\text{-}1^+$ myeloid cell accumulation influenced by the presence and size (volume) of autochthonous primary mammary tumour growth (Fig. 6). In contrast, in dTg mice, splenomegaly and $CD11b^+Gr\text{-}1^+$ myeloid cell production were significantly dampened regardless of tumour volume, which strengthens the hypothesis that IRF-8 plays an important role in constraining such haematopoietic changes.

Also, in contrast to what was observed with the $CD11b^+Gr\text{-}1^+$ population, the absolute numbers of $CD4^+$ T cells, $CD8^+$ T cells and NK cells did not significantly vary with tumour volume in both sTg MTAG and dTg mice. The absolute number of $B220^+$ B cells, however, was significantly higher ($P = 0.006$) in sTg MTAG *versus* dTg mice at just one level of tumour load ('med'). Furthermore, there were no significant differences in the total number of splenocytes, as well as the percentages and absolute numbers of these various lymphoid and myeloid subsets between wild-type and IRF-8 sTg mice. This suggested no adverse impact of the IRF-8 transgene on these haematopoietic compartments. Therefore, compared with sTg MTAG mice, transgenic expression of IRF-8 in MTAG mice seemed to constrain the tendency toward tumour-induced splenomegaly and $CD11b^+Gr\text{-}1^+$ myelopoiesis.

Discussion

$CD11b^+Gr\text{-}1^+$ MDSC are potentially important negative regulators of host immunosurveillance and antitumour activity. Therefore, efforts to understand their development or function may aid in the design of therapies that impede their involvement, thereby enhancing antitumour immunity. We tested the hypothesis that IRF-8 controls the development/expansion of tumour-induced $CD11b^+Gr\text{-}1^+$ cells. This notion stemmed from the original discovery that IRF-8 is essential for normal myeloid cell development, differentiation and function [14–19]. Consequently, if IRF-8 expression becomes altered during tumour growth or progression, this may have profound consequences on normal myelopoiesis and the accumulation of $CD11b^+Gr\text{-}1^+$ cells. In fact, IRF-8-deficiency in null mice causes a myeloproliferative disorder, including the emergence and expansion of $CD11b^+Gr\text{-}1^+$ myeloid

No claim to original US Government work
Journal compilation © 2009 Foundation for Cellular and Molecular Medicine/Blackwell Publishing Ltd

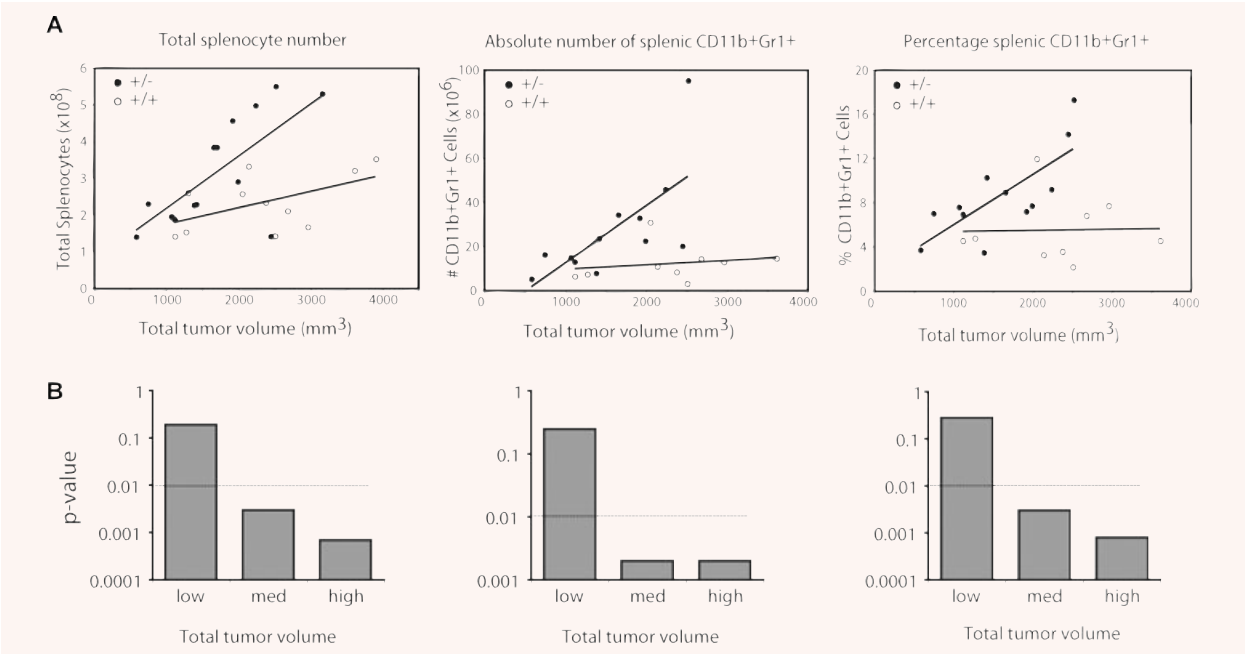

Fig. 6 Transgenic expression of IRF-8 reduces splenic CD11b$^+$Gr-1$^+$ cells in a spontaneous tumour model of mammary carcinoma. (**A**): The role of IRF-8 in the production of tumour-induced CD11b$^+$Gr-1$^+$ cells was analysed in a dTg mouse model as described in Fig. 5. Here, tumour-bearing sTg MTAG mice (denoted as '+/–') were compared to dTg mice (denoted as '+/+') for changes in the percentages and absolute numbers of splenic CD11b$^+$Gr-1$^+$ cells, as well as total splenocytes as a function of overall tumour load. As noted in Fig. 5, since transgenic expression of IRF-8 had no significant impact on tumour growth in dTg mice, both sTg and dTg groups were compared in an age- and littermate-matched fashion. It is also important to note that alterations in these haematopoietic parameters were not observed in IRF-8 sTg mice as compared to wild-type mice (not shown). Each data point represents data from an individual mouse. (**B**) Statistical summary of the data illustrated in the (**A**), whereby 'low, med (medium) and high' overall tumour loads reflected tumour volumes of approximately 1300, 2000 and 2500 mm^3, respectively, in sTg and dTg mice. Horizontal dashed line represents the statistical cut-off.

populations. The loss of IRF-8 in tumour-induced CD11b$^+$Gr-1$^+$ cells may also have important implications for the production of IRF-8-dependent cytokines, such as IL-12 [18, 33], which if reduced or inhibited could further compromise host–tumour immunosurveillance.

In this study, we examined whether: (*i*) IRF-8 expression in the CD11b$^+$Gr-1$^+$ population was down-regulated as a consequence of tumour growth and (*ii*) IRF-8 expression played a causal role in the emergence of tumour-induced CD11b$^+$Gr-1$^+$ cells *in vivo*. The approach taken to explore a mechanistic role of IRF-8 in the regulation of this myeloid population *in vivo* was to produce an IRF-8 Tg mouse. In this model, IRF-8 was transcriptionally regulated *via* the CMV promoter, and we focused our efforts on the consequences of tumour-induced alterations in the spleen, which included the induction of splenomegaly and an increase in the frequency/absolute numbers of splenic CD11b$^+$Gr-1$^+$ cells. The prediction was if tumour growth altered IRF-8 expression, and IRF-8 levels were important for the development or accumulation of the CD11b$^+$Gr-1$^+$ cell population, then tumour-bearing IRF-8 (dTg) mice would be more refractory to changes in the frequencies of these cells.

In addition to the well-characterized 4T1 mammary tumour model [21–23], we made use of the MTAG mouse model of autochthonous mammary carcinoma [24–28] to address specific aspects of the relationship between IRF-8 and CD11b$^+$Gr-1$^+$ myelopoiesis. As expected, 4T1 tumour growth led to profound splenomegaly, which was predominately attributed to the accumulation of CD11b$^+$Gr-1$^+$ cells. Similar findings have also been recently reported in the MTAG model [25, 26]. Functional studies verified that these cells were immunosuppressive, as judged by their ability to inhibit TCR-mediated lymphoproliferation *in vitro*. Moreover, in both the 4T1 and MTAG models, we observed an inverse relationship between IRF-8 expression and the emergence of these tumour-induced CD11b$^+$Gr-1$^+$ cells. The exact mechanisms that alter IRF-8 expression, however, remain unclear but may reflect the types and/or quantities of TDF. For instance, several studies have reported that different tumours secrete various factors that potentially modulate the generation, differentiation and/or function of CD11b$^+$Gr-1$^+$ cells, namely VEGF, GM-CSF, CSF-1, IL-10, PGE_2 and/or IL-1 [4, 5, 8, 22, 32, 36, 37]. Thus, future work is needed to evaluate the relative contribution of these and/or other TDF that potentially affect IRF-8 expression in these myeloid populations.

No claim to original US Government work
Journal compilation © 2009 Foundation for Cellular and Molecular Medicine/Blackwell Publishing Ltd

Nonetheless, it was clear that transgenic expression of IRF-8 in MTAG mice (through the use of the dTg model) significantly reduced the propensity for splenomegaly and $CD11b^+Gr\text{-}1^+$ myelopoiesis. This indicates that IRF-8 plays a causal role in the tumour-directed process of $CD11b^+Gr\text{-}1^+$ cell induction and/or expansion. It is important to emphasize that in this study we focused on IRF-8-induced changes in splenic and bone marrow compartments of tumour-bearing mice, where counterpart control cell populations could be similarly isolated from non-tumour-bearing mice for comparison. Future studies are warranted to evaluate IRF-8 expression levels in tumour-infiltrating myeloid populations, as well as the functional impact of IRF-8 overexpression on MDSC activity and apoptotic phenotype. Additionally, although earlier studies have implicated a role for Stat3 activation in the development of these cells [1, 38], follow-up investigations are needed to reveal the precise molecular or biochemical relationship between these two transcription factors, IRF-8 and Stat3.

Despite the fact that IRF-8 expression in autochthonous tumour-bearing dTg mice resulted in a reversal to a near normal frequency of $CD11b^+Gr\text{-}1^+$ cells, there was no significant effect on primary tumour growth. It is possible, however, that the reduction in $CD11b^+Gr\text{-}1^+$ cells *per se* may be insufficient to affect tumour growth or progression and that additional host factors or mechanisms acting in concert with alterations in these cells may be required to maximally inhibit tumour growth. This notion is consistent with other tumour studies, revealing that biologic- or immune-based therapies mediate stronger antitumour effects when combined with strategies that eliminate MDSC or inhibit their suppressive function [39–43]. It is also possible that the lack of effect on tumour growth in dTg mice may be due to inadequate numbers of immune cells that infiltrate these tumours. This contention is supported by preliminary histopathological findings of tumours derived from sTg MTAG and dTg mice, which revealed low numbers of inflammatory cell infiltrates, as well as apoptosis in both groups of tumours.

Although further studies are necessary to explore the mechanism(s) underlying the lack of immune cell infiltration, our results in dTg mice demonstrated that transgenic IRF-8 expression affected the haematopoietic system and functioned as a suppressor of tumour-induced $CD11b^+Gr\text{-}1^+$ cell development/accumulation. Interestingly, the cytokine/chemokine profile of $CD11b^+Gr\text{-}1^+$ cells of tumour-bearing IRF-8 transgenic mice returned to a more 'normal', non-tumour-bearing phenotype. In terms of secreted IL-12 levels, there was a tendency toward higher amounts produced by $CD11b^+Gr\text{-}1^+$ myeloid cells of the IRF-8 transgenic group compared with the non-transgenic group (manuscript submitted). Future studies are also necessary to investigate additional functional aspects of IRF-8 overexpression, such as the effect of IRF-8 on MDSC activity, as well as their apoptotic phenotype. Taken collectively, this study demonstrates for the first time that differential IRF-8 expression plays an important role in the development and accumulation of tumour-induced $CD11b^+Gr\text{-}1^+$ cells, which may have important implications for the design of improved anti-cancer combination therapies.

Acknowledgements

We thank Drs. Keiko Ozato (NICHD, NIH) for providing the IRF-8 plasmid, Sandra Gendler (Mayo Clinic) for originally providing the B6-MTAG mice and Lionel Feigenbaum (SAIC/NCI) for assistance with the production of the IRF-8 transgenic mouse. This research was supported (in part) by the Intramural Research Program of the NIH, National Cancer Institute, Center for Cancer Research. This work was also supported in part by RCPI Institutional Funding (to S.I.A.). K Liu is supported by Grant ROI CA 133085 from the National Cancer Institute/NIH.

References

1. **Wang T, Niu G, Kortylewski M, *et al.*** Regulation of the innate and adaptive immune responses by Stat-3 signaling in tumor cells. *Nature Med.* 2004; 10: 48–54.
2. **Rabinovich GA, Gabrilovich D, Sotomayor EM.** Immunosuppressive strategies that are mediated by tumor cells. *Annu Rev Immunol.* 2007; 25: 267–96.
3. **Stewart TJ, Greeneltch KM, Lutsiak ME, *et al.*** Immunological responses can have both pro- and antitumour effects: implications for immunotherapy. *Expert Rev Mol Med.* 2007; 9: 1–20.
4. **Nagaraj S, Gabrilovich DI.** Myeloid-derived suppressor cells. *Adv Exp Med Biol.* 2007; 601: 213–23.
5. **Kusmartsev S, Gabrilovich DI.** Role of immature myeloid cells in mechanisms of immune evasion in cancer. *Cancer Immunol Immunother.* 2006; 55: 237–45.
6. **Almand B, Clark JI, Nikitina E, *et al.*** Increased production of immature myeloid cells in cancer patients: a mechanism of immunosuppression in cancer. *J Immunol.* 2001; 166: 678–89.
7. **Filipazzi P, Valenti R, Huber V, *et al.*** Identification of a new subset of myeloid suppressor cells in peripheral blood of melanoma patients with modulation by a granulocyte-macrophage colony-stimulation factor-based antitumor vaccine. *J Clin Oncol.* 2007; 25: 2546–53.
8. **Ochoa AC, Zea AH, Hernandez C, *et al.*** Arginase, prostaglandins, and myeloid-derived suppressor cells in renal cell carcinoma. *Clin Cancer Res.* 2007; 13: 721s–6s.
9. **Schmielau J, Finn OJ.** Activated granulocytes and granulocyte-derived hydrogen peroxide are the underlying mechanism of suppression of t-cell function in advanced cancer patients. *Cancer Res.* 2001; 61: 4756–60.
10. **Zea AH, Rodriguez PC, Atkins MB, *et al.*** Arginase-producing myeloid suppressor cells in renal cell carcinoma patients: a mechanism of tumor evasion. *Cancer Res.* 2005; 65: 3044–8.
11. **Terabe M, Matsui S, Park JM, *et al.*** Transforming growth factor-beta production and myeloid cells are an effector mechanism through which CD1d-restricted T cells block cytotoxic T lymphocyte-mediated tumor immunosurveillance: abrogation prevents tumor recurrence. *J Exp Med.* 2003; 198: 1741–52.

No claim to original US Government work
Journal compilation © 2009 Foundation for Cellular and Molecular Medicine/Blackwell Publishing Ltd

12. **Bronte V, Zanovello P.** Regulation of immune responses by L-arginine metabolism. *Nature Rev.* 2005; 5: 641–54.
13. **Yang L, DeBusk LM, Fukuda K, *et al.*** Expansion of myeloid immune suppressor $Gr^{+}CD11b^{+}$ cells in tumor-bearing host directly promotes tumor angiogenesis. *Cancer Cell.* 2004; 6: 409–21.
14. **Nagamura-Inoue T, Tamura T, Ozato K.** Transcription factors that regulate growth and differentiation of myeloid cells. *Int Rev Immunol.* 2001; 20: 83–105.
15. **Schiavoni G, Mattei F, Borghi P, *et al.*** ICSBP is critically involved in the normal development and trafficking of Langerhans cells and dermal dendritic cells. *Blood.* 2004; 103: 2221–8.
16. **Tsujimura H, Nagamura-Inoue T, Tamura T, *et al.*** IFN consensus sequence binding protein/IFN regulatory factor-8 guides bone marrow progenitor cells toward the macrophage lineage. *J Immunol.* 2002; 169: 1261–9.
17. **Holtschke T, Lohler J, Kanno Y, *et al.*** Immunodeficiency and chronic myelogenous leukemia-like syndrome in mice with a targeted mutation of the ICSBP gene. *Cell.* 1996; 87: 307–17.
18. **Masumi A, Tamaoki S, Wang IM, *et al.*** IRF-8/ICSBP and IRF-1 cooperatively stimulate mouse IL-12 promoter activity in macrophages. *FEBS Lett.* 2002; 531: 348–53.
19. **Tamura T, Ozato K.** ICSBP/IRF-8: its regulatory roles in the development of myeloid cells. *J Interferon Cytokine Res.* 2002; 22: 145–52.
20. **Gabriele L, Phung J, Fukumoto J, *et al.*** Regulation of apoptosis in myeloid cells by interferon consensus sequence-binding protein. *J Exp Med.* 1999; 190: 411–21.
21. **Aslakson CJ, Miller FR.** Selective events in the metastatic process defined by analysis of the sequential dissemination of subpopulations of a mouse mammary tumor. *Cancer Res.* 1992; 52: 1399–405.
22. **Bunt SK, Yang L, Sinha P, *et al.*** Reduced inflammation in the tumor microenvironment delays the accumulation of myeloid-derived suppressor cells and limits tumor progression. *Cancer Res.* 2007; 67: 10019–26.
23. **Sinha P, Okoro C, Foell D, *et al.*** Proinflammatory s100 proteins regulate the accumulation of myeloid-derived suppressor cells. *J Immunol.* 2008; 181: 4666–75.
24. **Guy CT, Cardiff RD, Muller WJ.** Induction of mammary tumors by expression of polyomavirus middle T oncogene: a transgenic mouse model for metastatic disease. *Mol Cell Biol.* 1992; 12: 954–61.
25. **Stewart TJ, Abrams SI.** Altered immune function during long-term host-tumor interactions can be modulated to retard autochthonous neoplastic growth. *J Immunol.* 2007; 179: 2851–9.
26. **Stewart TJ, Lutsiak ME, Abrams SI.** Immune consequences of protracted host-tumor interactions in a transgenic mouse model of mammary carcinoma. *Cancer Invest.* 2008; 26: 237–49.
27. **Maglione JE, Moghanaki D, Young LJ, *et al.*** Transgenic polyoma middle-T mice model premalignant mammary disease. *Cancer Res.* 2001; 61: 8298–305.
28. **Lin EY, Jones JG, Li P, *et al.*** Progression to malignancy in the polyoma middle T oncoprotein mouse breast cancer model provides a reliable model for human diseases. *Am J Pathol.* 2003; 163: 2113–26.
29. **Lin EY, Pollard JW.** Tumor-associated macrophages press the angiogenic switch in breast cancer. *Cancer Res.* 2007; 67: 5064–6.
30. **Chen D, Xia J, Tanaka Y, *et al.*** Immunotherapy of spontaneous mammary carcinoma with fusions of dendritic cells and mucin 1-positive carcinoma cells. *Immunology.* 2003; 109: 300–7.
31. **Greeneltch KM, Haudenschild CC, Keegan AD, *et al.*** The opioid antagonist naltrexone blocks acute endotoxic shock by inhibiting tumor necrosis factor-alpha production. *Brain Behav Immun.* 2004; 18: 476–84.
32. **Serafini P, Carbley R, Noonan KA, *et al.*** High-dose granulocyte-macrophage colony-stimulating factor-producing vaccines impair the immune response through the recruitment of myeloid suppressor cells. *Cancer Res.* 2004; 64: 6337–43.
33. **Wang IM, Contursi C, Masumi A, *et al.*** An IFN-gamma-inducible transcription factor, IFN consensus sequence binding protein (ICSBP), stimulates IL-12 p40 expression in macrophages. *J Immunol.* 2000; 165: 271–9.
34. **Huang B, Pan PY, Li Q, *et al.*** Gr-1+CD115+ immature myeloid suppressor cells mediate the development of tumor-induced T regulatory cells and T-cell anergy in tumor-bearing host. *Cancer Res.* 2006; 66: 1123–31.
35. **Sinha P, Clements VK, Bunt SK, *et al.*** Cross-talk between myeloid-derived suppressor cells and macrophages subverts tumor immunity toward a type 2 response. *J Immunol.* 2007; 179: 977–83.
36. **Rodriguez PC, Hernandez CP, Quiceno D, *et al.*** Arginase I in myeloid suppressor cells is induced by COX-2 in lung carcinoma. *J Exp Med.* 2005; 202: 931–9.
37. **Sinha P, Clements VK, Fulton AM, *et al.*** Prostaglandin E2 promotes tumor progression by inducing myeloid-derived suppressor cells. *Cancer Res.* 2007; 67: 4507–13.
38. **Nefedova Y, Huang M, Kusmartsev S, *et al.*** Hyperactivation of STAT3 is involved in abnormal differentiation of dendritic cells in cancer. *J Immunol.* 2004; 172: 464–74.
39. **Kusmartsev S, Cheng F, Yu B, *et al.*** All-trans-retinoic acid eliminates immature myeloid cells from tumor-bearing mice and improves the effect of vaccination. *Cancer Res.* 2003; 63: 4441–9.
40. **Serafini P, Meckel K, Kelso M, *et al.*** Phosphodiesterase-5 inhibition augments endogenous antitumor immunity by reducing myeloid-derived suppressor cell function. *J Exp Med.* 2006; 203: 2691–702.
41. **De Santo C, Serafini P, Marigo I, *et al.*** Nitroaspirin corrects immune dysfunction in tumor-bearing hosts and promotes tumor eradication by cancer vaccination. *Proc Natl Acad Sci USA.* 2005; 102: 4185–90.
42. **Suzuki E, Kapoor V, Jassar AS, *et al.*** Gemcitabine selectively eliminates splenic Gr-1+/CD11b+ myeloid suppressor cells in tumor-bearing animals and enhances antitumor immune activity. *Clin Cancer Res.* 2005; 11: 6713–21.
43. **Shojaei F, Wu X, Malik AK, *et al.*** Tumor refractoriness to anti-VEGF treatment is mediated by CD11b+Gr1+ myeloid cells. *Nat Biotechnol.* 2007; 25: 911–20.

No claim to original US Government work
Journal compilation © 2009 Foundation for Cellular and Molecular Medicine/Blackwell Publishing Ltd